Characterization of silk gland ribosomes from a bivoltine caddisfly, *Stenopsyche marmorata*: translational suppression of a silk protein in cold conditions[1]

Takaomi Nomura [a]*, **Miho Ito** [a], **Mai Kanamori** [a], **Yuta Shigeno** [a], **Toshio Uchiumi** [b], **Ryoichi Arai** [a,c], **Masuhiro Tsukada** [a], **Kimio Hirabayashi** [a,d], **and Kousaku Ohkawa** [e]

[a] Division of Applied Biology, Faculty of Textile Science and Technology, Shinshu University, Ueda 386-8567, Japan

[b] Department of Biology, Faculty of Science, Niigata University, Niigata 950-2181, Japan

[c] Institute for Biomedical Sciences, Interdisciplinary Cluster for Cutting Edge Research, Shinshu University, Matsumoto 390-8621, Japan

[d] Institute of Mountain Science, Interdisciplinary Cluster for Cutting Edge Research, Shinshu University, Minamiminowa, Nagano 399-4598, Japan

[e] Institute for Fiber Engineering, Interdisciplinary Cluster for Cutting Edge Research, Shinshu University, Ueda 386-8567, Japan

* Corresponding author. E-mail address: nomurat@shinshu-u.ac.jp

---

[1] **Abbreviations**: DDBJ, DNA data bank of Japan; SDS-PAGE, sodium dodecyl sulfate; Smsp, *Stenopsyche marmorata* silk protein; rRNA, ribosomal RNA; CBB, Coomassie brilliant blue; TOR, target of rapamycin; SG, stress granule; SDG, sucrose density gradient; NTE, N-terminal extension; EF-mix, elongation factor mix

ABSTRACT

Larval *Stenopsyche marmorata* constructs food capture nets and fixed retreats underwater using self-produced proteinaceous silk fibers. In the Chikuma River (Nagano Prefecture, Japan) *S. marmorata* has a bivoltine life cycle; overwintering larvae grow slowly with reduced net spinning activity in winter. We recently reported constant transcript abundance of *S. marmorata* silk protein 1 (Smsp-1), a core *S. marmorata* silk fiber component, in all seasons, implying translational suppression in the silk gland during winter. Herein, we prepared and characterized silk gland ribosomes from seasonally collected *S. marmorata* larvae. Ribosomes from silk glands immediately frozen in liquid nitrogen (LN_2) after dissection exhibited comparable translation elongation activity in spring, summer, and autumn. Conversely, silk glands obtained in winter did not contain active ribosomes and Smsp-1. Ribosomes from silk glands immersed in ice-cold physiological saline solution for approximately 4 h were translationally inactive, despite summer collection and Smsp-1 expression. The ribosomal inactivation occurs because of defects in the formation of 80S ribosomes, presumably due to splitting of 60S subunits containing 28S rRNA with central hidden break, in response to cold stress. These results suggest a novel-type ribosome-regulated translation control mechanism.

1. Introduction

Extreme environmental changes (pH, temperature, osmolality, and nourishment) represent a serious concern for all organisms; hence, organisms have acquired effective strategies for adaptation and survival under various stress conditions. Stresses affect global cellular metabolism and lead to transient cell growth and proliferation arrest, which are directly associated with increasing changes in global gene expression [1]. Gene transcription and translation are important and energy-expensive cellular processes, and the biogenesis of ribosomes, large RNA-protein complexes with a role of core translation machinery, also consumes substantial metabolic energy. Ribosome biogenesis requires up to 40% and 60–80% of the total energy production in growing bacterial and eukaryotic cells, respectively [2,3]. Therefore, stress-related translation control is a key energy-saving strategy.

In bacteria, the low nutrient-induced translationally inactive 100S ribosome (70S ribosome dimer) formation represents an excellent economic system that inhibits translation and stably maintains ribosomes in cells until environment conditions improve [4]. A similar mechanism (inactive 110S ribosome via 80S ribosome dimerization) has been detected in eukaryotic cells, although the details are unknown [5]; conversely, up-/down-regulation of the translation initiation step via eukaryotic translation initiation factor 2α (eIF2α) and target of rapamycin (TOR) signaling pathway is a well-known global translation control mechanism [6]. Additionally, translation initiation inhibition, although limited for housekeeping mRNAs, allows stalled translational pre-initiation complexes to accumulate and aggregate, resulting in cellular RNA-protein particle, so-called stress granule (SG), formation [7]. Because SGs typically contain housekeeping mRNA, small ribosomal subunits (40S), translation initiation factors, and poly-A binding protein, SGs may facilitate selective protection of housekeeping mRNAs and provide temporary storage for immediate translation resumption. SGs disassemble and sequestered mRNAs return to the cytosol, once stress is relieved [8].

The caddisfly (Trichoptera) is a representative aquatic insect, for which larvae and pupae are found in freshwater environments (streams, rivers, lakes, and ponds). Annulipalpia, a suborder of Trichoptera, is known as the "fixed-retreat maker" or "net-spinning caddisfly;" the larvae spin adhesive silk fibers used to construct food capture nets and fixed retreats underwater [9-11]. *Stenopsyche marmorata* (Annulipalpia) commonly inhabits the main island (Honshu) of Japan and exhibits bivoltine life cycles [12]. The overwintering larvae grow slower than the summer generation larvae; the estimated mean instantaneous growth rate per individual of the former is less than half of the latter [13]. Bivoltine type of Hydropsyche (Annulipalpia) larvae exhibited reduced net-spinning activity during winter in response to lower water temperatures and shorter photoperiod [14].

We previously identified four major *S. marmorata* silk proteins (Smsp-1–4) in larval silk glands and obtained partial/complete amino acid and nucleic acid sequences [10,15-17]. Smsp-1 with a high molecular mass (>300 kDa) is a core silk fiber component [10,16,17]. We additionally noticed substantial season-independent Smsp-1 transcript abundance in the silk glands [15]. Therefore, we speculated that Smsp-1 synthesis in *S. marmorata* larval silk glands is down-regulated at the translation level during winter; we biochemically characterized silk gland ribosomes from seasonally collected *S. marmorata* larvae and discussed adaptive translational regulation for external temperature changes.

2. Materials and Methods

2.1 Ribosomes, ribosomal RNA, and silk proteins

Fifth instar larvae of *S. marmorata* were collected in the middle of the Chikuma River near the Komaki Bridge in Nagano Prefecture, Japan, during April (spring), June (summer), September (autumn), and December (winter) 2008–2010. Larval silk glands were immediately frozen in liquid nitrogen (LN_2) or immersed in ice-cold physiological saline

solution for approximately 4 h during dissection (ice-cold) and stored at −80°C until use. Membrane-free crude ribosomes were prepared from soluble cellular silk gland extracts (S10) via ultracentrifugation (50,000 rpm, 18 h; Hitachi P70AT rotor). Purified ribosomes were similarly recovered after puromycin treatment in the presence of 0.5 M KCl [18] (Fig. S1). Similar to *B*. *mori* silk glands, all ribosome samples yielded 18-20 A_{260} (absorbance at 260 nm) units/g of silk gland.

Protein components of 0.3 A_{260} units of purified ribosomes were separated on SDS-PAGE on 16.5% (w/v) polyacrylamide gels followed by Coomassie brilliant blue (CBB) staining. Ribosomal RNA (rRNA) was obtained from purified ribosomes via phenol extraction. rRNA samples (250 ng) were incubated at 65°C for 5 min, chilled on ice, immediately analyzed by denaturing agarose gel electrophoresis [19], and visualized with SYBR Gold (Thermo Fisher Scientific, USA). Under native conditions, the same rRNA samples were analyzed without thermal treatment. Silk proteins were obtained from 8 M urea extracts of insoluble silk gland residues (P10) (Fig. S1), analyzed by SDS-PAGE on 3–20 % (w/v) polyacrylamide gradient gels, and visualized with CBB staining.

2.2 Ribosome functional assay

Poly(U)-dependent polyphenylalanine synthesis was performed at 37°C for 10 min in a 75 µl solution containing 10 pmol of purified ribosomes, 40 pmol of [^{14}C] Phe-tRNA (400 cpm/pmol), 10 µg of poly(U), 0.25 mM GTP, 5 mM MgCl$_2$, 100 mM NH$_4$Cl, 0.2 mM dithiothreitol, and 50 mM Tris-HCl (pH 7.5) in the presence of 200 µg of S200 fraction (EF-mix) from *B*. *mori* silk gland cell lysate [18]. Measurements were performed several times; P values were calculated using a two-tailed Welch's t-test.

2.3 Ribosome sedimentation assay

For 80S ribosome analysis, 10 pmol of purified ribosomes were incubated at 37°C for 10 min in 5 mM $MgCl_2$, 25 mM KCl, 5 mM 2-mercaptoethanol, and 20 mM Tris-HCl (pH 7.6). The solution was overlaid on a 15%–30% (w/v) sucrose gradient in the same buffer and centrifuged for 3 h at 40,000 rpm and 4°C in a Hitachi RPS65T rotor. Ribosomal subunits (60S and 40S) were similarly analyzed, except the solution contained 3 mM $MgCl_2$ and 300 mM KCl. After centrifugation, the gradient was pumped from the bottom of the tube using a peristaltic pump under simultaneous and continuous A_{260} monitoring.

2.4 Next-generation sequencing transcriptome analysis of silk glands

Total RNA was isolated from *S. marmorata* larval silk glands frozen in LN_2 using an ISOGEN-LS (Nippon Gene, Japan) according to the manufacturer's instructions. After determining RNA quantity and quality, RNA-seq libraries were prepared using a TruSeq RNA sample prep kit (Illumina, USA) according to standard protocols. Quality-checked libraries were sequenced with 100 bp paired-end reads on an Illumina HiSeq2000 instrument (Illumina, USA). Quality control analysis of FASTQ raw data was performed on Maser web-based analysis pipeline, Cell Innovation program (National Institute of Genetics; http://cell-innovation.nig.ac.jp), and was achieved by (i) removing duplicated reads, (ii) trimming adapter sequences and 9 bases from 5′ ends, and (iii) filtering low-quality reads. Quality-controlled reads were assembled *de novo* using Trinity program, DDBJ Read Annotation pipeline (http://p.ddbj.nig.ac.jp/pipeline) [20,21], which generated 21,517 contigs of >200 bp with a N50 of 842 bp. Functional annotation of all contigs was based on best BlastX (Uniprot/Swiss-prot) and BlastN (NCBI/NR) hits on the Maser analysis pipeline. Contigs_04358 and 05690 contained full-length 5.8S-28S rRNA and ribosomal protein L23a genes, respectively; each sequence was registered in DDBJ under accession numbers LC094265 and LC094266.

3. Results and discussion

3.1 Seasonal translational activity in larval silk glands

We previously demonstrated constant abundance of Smsp-1 mRNA in *S. marmorata* larval silk glands collected even in winter when larval net-spinning activity decreased [15]. To further investigate the molecular details of season-dependent translation regulation in *S. marmorata*, we analyzed the ribosomes. Translationally active ribosomes were isolated from immediately LN$_2$-frozen silk glands of *S. marmorata* larvae collected in spring, summer, and autumn (Fig. 1A). In contrast, ribosomes isolated from silk glands collected in winter exhibited remarkably reduced translation activity (Fig. 1A, winter/LN$_2$). In addition, inactive ribosomes were also obtained from ice-cold silk glands of the summer larvae (Fig. 1A, summer/ice-cold) although active ribosomes were prepared from *B. mori* silk glands via the same procedure [18] (Fig. 1A, *B. mori*). We further analyzed silk proteins in *S. marmorata* larval silk glands by SDS-PAGE analysis. No Smsp-1 was detected (Fig. 1B, lane 1) in winter, despite mRNA presence [15]. This result is consistent with very low activity of the ribosomes prepared from the winter silk glands (Fig. 1A, winter/LN$_2$). *S. marmorata* larvae appear to suspend translating Smsp-1 mRNA by inactivating ribosomes during winter. In summer, Smsp-1 was detected in silk glands prepared under ice-cold conditions (summer/ice-cold) (Fig. 1B, lane 2). These imply that the cold conditions trigger down-regulation of Smsp-1 translation.

3.2 Ribosome particle characterization

Typical eukaryotic ribosomes have a sedimentation coefficient of 80S, and are composed of 60S (large) and 40S (small) subunits. We examined ribosome profiles using sucrose density gradient (SDG) analysis to explore differences between active and inactive ribosomes

from *S. marmorata* silk glands (Fig. 2). *B. mori* ribosomes exhibited typical sedimentation patterns with a single 80S ribosome peak and double peaks corresponding to 60S and 40S subunits in the presence of low (50 mM KCl/5 mM MgCl$_2$; Fig. 2A, dotted line) and high (300 mM KCl/3 mM MgCl$_2$; Fig. 2B, dotted line) ionic strengths, respectively. Similar patterns were observed in active ribosomes prepared from summer silk glands under both ionic strength conditions (Fig. 2A and B, red). Conversely, 80S peak intensity drastically decreased in inactive ribosomes prepared from winter silk glands despite low ionic strength conditions (Fig. 2A, blue), indicating translation activity correlation with 80S ribosome formation. Significant increases in 40S subunits and smaller sedimentation particle generation (estimated at 27-30S) in the same ribosomes were accompanied by a decrease in 60S subunits under high ionic conditions (Fig. 2B, blue); an identical pattern was observed in ribosomes prepared from ice-cold summer silk glands (Fig. S2). These results suggest that cold stress induces splitting 60S subunits into at least two particles with 40S and 27-30S sedimentation coefficients, blocking 80S ribosome formation. We unsuccessfully attempted to determine whether these peaks included some of the 60S subunits, although it appeared likely that 40S subunits remained intact in cold conditions (Fig. 2B, blue). We inferred that small ribosomal subunits were stably retained in SGs together with Smsp-1 mRNAs under cold stress conditions.

We proceeded to analyze ribosomal components, proteins and RNAs. Although with slight differences, SDS-PAGE analysis (Fig. 3A) revealed similar 80S ribosome protein patterns among active summer (summer/LN$_2$, lane 1), inactive winter (winter/LN$_2$, lane 2), and inactive summer (summer/ice-cold, lane 3) samples. Agarose gel electrophoresis of rRNAs prepared from the same ribosome samples failed to reveal differences (Fig. S3). These results imply that ribosomal protein assembly on rRNAs occurs in similar manner, regardless of ribosome activity.

We were interested in the disappearance of the 28S rRNA bands of *S. marmorata* (Sm) and *B. mori* (Bm) and enhancement of the 18S rRNA bands under both native and denaturing conditions (Fig. 3B, lane Bm and Sm), which appeared not to result from artificial cleavage, because a distinct *Rattus norvegicus* (Rn) 28S rRNA band was detected in the same gels (Fig. 3B, lane Rn). These results suggest that *S. marmorata* (Trichoptera) has central cleavage of 28S rRNA molecule, a "hidden break" often found in protostomes such as *B. mori* (Lepidoptera) [22].

3.3 Prediction of the central hidden break site in 28S rRNA

The precise central hidden break site has been determined for some protostomia species including *Schistosoma mansoni* (blood fluke), *Trichinella spirallis* (trichina worm), *Drosophila melanogaster* (fruit fly), *Sciara coprophila* (fungus gnat), and *B. mori* (silkworm), and is located at expansion segment 19L (ES19L) or divergent domain D7a and variable region V9, in the Domain III of 28S rRNA. ES19L is a branching helix evolutionally inserted into helix52, a common helical trunk in bacterial 23S rRNA [23-25]. A recent cryo-electron microscopy structural analysis of *D. melanogaster* and *Homo sapiens* (human) 80S ribosomes revealed that the 28S rRNA of *D. melanogaster*, but not of *H. sapiens*, was separated into two fragments, 28Sα and 28Sβ, by splicing out 45 bases at the central hidden break site (Fig. S4) [26]. We obtained a complete 28S rRNA sequence via *de novo* transcriptome analysis of the *S. marmorata* silk gland (contig_04358); this allowed construction of a secondary structure model of *S. marmorata* ES19L (Fig. 4A), which is similar to that of *B. mori* (Fig. 4B), *D. melanogaster*, (Fig. 4C), and *H. sapiens* (Fig 4D). Hidden break sites are predicted to exist in a large loop next to the ES19L stem (Fig. 4A-C), although this does not occur in *H. sapiens* rRNA (Fig. 4D). When and how 28S rRNA is processed to generate the central hidden break is unclear. Several researchers have proposed

a relationship between ribosomal protein L23a (L25 in yeast) and hidden break processing because most organisms with a central hidden break harbor a flexible histone H1-like N-terminal extension (NTE) in L23a; the NTE of L23a, although its structure cannot be visualized, appears to be located adjacent to the central hidden break site (Fig. S4) [26-29]. *S. marmorata* L23a (contig_05690 in our transcripts) contains the NTE of approximately 180 amino acids (full-length is 326 amino acids) with relatively high homology to corresponding part in *B. mori* and *D. melanogaster*, but not in *H. sapiens* (Fig. 4E).

3.4 Relationship between fragmented 28S rRNA and translation control

The central hidden break of 28S rRNA probably plays an important role in ribosome function because processing is widely observed in protostomes [22]; however, little is known about its biological and physiological significance. Besides the central hidden break, large subunit rRNA (28S/23S) fragmentation has been detected in various living cells and organelles [30-39]. Azpurua *et al.* recently revealed that 28S rRNA of naked mole-rat, a subterranean rodent, is cleaved into two fragments within ES15L (D6) region; naked mole-rat cells have a 4–10-fold higher global translation fidelity relative to mouse cells, despite equivalent translation rates [30]. Additionally, the chloroplast ribosomes of an *Arabidopsis thaliana nara12-1* mutant, which exhibits defective chloroplast 23S rRNA fragmentation processing, have dysfunctional translation elongation [31], thereby suggesting 28S/23S rRNA fragmentation is a translation control strategy in various organisms, regardless of its variable effects. Therefore, it is a leading hypothesis that the central hidden break involves splitting of 60S subunits in *S. marmorata* silk glands exposed to cold stress and, thus, diminished translation of Smsp-1 mRNA. Ribosome biogenesis and protein synthesis require considerable energy and are, thus, down-regulated to avoid wasteful energy consumption under unfavorable growth and proliferation conditions [2,3]. Limited 60S subunit destruction,

which would allow immediate regeneration of mature 60S subunits via split particle reassembly in response to improved conditions, is energetically advantageous. This process appears to be a novel-type ribosomal-regulated translational control involving the central hidden break of 28S rRNA in response to cold stress.

Now, the question is why do *B. mori* ribosomes from ice-cold treated silk glands exhibit normal translation activity despite the central hidden break in 60S subunits? The reason is still unknown; however, a possible reason is that *B. mori* is a domesticated animal and does not overwinter at the larval stage. In the fields of molecular and cellular biology, most studies have used laboratory organisms (rat, mouse, *D. melanogaster*, and *B. mori*). Moreover, future studies of wild organisms such as *S. marmorata* will give further insights for biological function and regulation in nature.

References

[1]   L. López-Maury, S. Marguerat, J. Bähler, Tuning gene expression to changing environments: from rapid responses to evolutionary adaptation, Nat. Rev. Genet. 9 (2008) 583-593.

[2]   B. A. Maguire, Inhibition of Bacterial ribosome assembly: a suitable drug target?, Microbiol. Mol. Biol. Rev. 73 (2009) 22–35.

[3]   T. Moss, V. Y. Stefanovsky, At the center of eukaryotic life, Cell 109 (2002) 545-548.

[4]   H. Yoshida, A. Wada, The 100S ribosome: ribosomal hibernation induced by stress, WIREs RNA 5 (2014) 723-732.

[5]   D. Krokowski, F. Gaccioli, M. Majumder, et al., Characterization of hibernating ribosomes in mammalian cells, Cell Cycle 10 (2011) 2691-2702.

[6]   S. Huch, T. Nissan, Interrelations between translation and general mRNA degradation in yeast, WIREs RNA 5 (2014) 747-763.

[7]   C. J. Decker, R. Parker, P-bodies and stress granules: possible roles in the control of translation and mRNA degradation, Cold Spring Harb. Perspect. Biol. 4 (2012) a012286.

[8]   N. Kedersha, G. Stoecklin, M. Ayodele, et al., Stress granules and processing bodies are dynamically linked sites of mRNP remodeling, J. Cell Biol. 169 (2005) 871–884.

[9]   J. M. Glime, Aquatic Insects: Holometabola - Trichoptera, Suborder Annulipalpia, Bryophyte Ecology Vol. 2 Bryological Interaction (2015) Chapter 11-11 (http://www.bryoecol.mtu.edu/).

[10]   K. Ohkawa, T. Nomura, R. Arai, et al., Characterization of Underwater Silk Proteins from Caddisfly Larva, *Stenopsyche marmorata*, in: T. Asakura, T. Miller (Eds.) Biotechnology of Silk, Biologically-Inspired Systems 5, Springer, Dordrecht, (2014) 107-122.

[11] M. Tsukada, M. M. Khan, E. Inoue, et al., Physical properties and structure of aquatic silk fiber from *Stenopsyche marmorata*, Int. J. Biol. Macromol. 46 (2010) 54-58.

[12] K. Gose, Life history and instar analysis of Stenopsyche griseipennis (Trichoptera), Jpn. J. Limnol. 31 (1970) 96-106 (in Japanese).

[13] K. Aoya, N. Yokoyama, Production of two species of *Stenopsyche* (Trichoptera: Stenopsychidae) in Tohoku district, Jpn. J. Limnol. 51 (1990) 249-260 (in Japanese).

[14] R. L. Fuller, R. J. Mackay, Field and laboratory studies of net spinning activity by *Hydropsyche* larvae (Trichoptera: Hydropsychidae), Can. J. Zool. 58 (1980) 2006-2014.

[15] X. Bai, M. Sakaguchi, Y. Yamaguchi, et al., Molecular cloning, gene expression analysis, and recombinant protein expression of novel silk proteins from larvae of a retreat-maker caddisfly, *Stenopsyche marmorata*, Biochem. Biophys. Res. Commun. 464 (2015) 814-9

[16] K. Ohkawa, Y. Miura, T. Nomura, et al., Long-range periodic sequence of the cement/silk protein of *Stenopsyche marmorata*: purification and biochemical characterisation, Biofouling 29 (2013) 357-367.

[17] K. Ohkawa, Y. Miura, T. Nomura, et al., Isolation of silk proteins from a caddisfly larva, *Stenopsyche marmorata*, J. Fiber Bioeng. Inform. 5 (2012) 125-137.

[18] T. Nomura, T. Uchiumi, M. Nakagaki, et al., A Covariant Change of the Two Highly Conserved Bases in the GTPase-associated Center of 28 S rRNA in Silkworms and Other Moths, J. Biol. Chem. 275 (2000) 35116-35121.

[19] T. Maseka, V. Vopalenskya, P. Suchomelovab, M. Pospiseka, Denaturing RNA electrophoresis in TAE agarose gels, Anal. Biochem. 336 (2005) 46–50.

[20] H. Nagasaki, T. Mochizuki, Y. Kodama, et al., DDBJ read annotation pipeline: a cloud computing-based pipeline for high-throughput analysis of next-generation sequencing data, DNA Res. 20 (2013) 383-90.

[21] M. G. Grabherr, B. J. Haas, M. Yassour, et al., Full-length transcriptome assembly from RNA-seq data without a reference genome, Nat. Biotechnol. 29 (2011) 644-652.

[22] H. Ishikawa, Evolution of ribosomal RNA, Comp. Biochem. Phy.siol. 58 B (1977) 1-7.

[23] D. S. Zarlenga, J. B. Dame, The identification and characterization of a break within the large subunit ribosomal RNA of *Trichinella spiralis*: comparison of gap sequences within the genus, Mol. Biochem. Parasitol. 45 (1992) 281-290.

[24] H. van Keulen, P. M. Mertz, P. T. LoVerde, et al., Characterization of a 54-nucleotide gap region in the 28S rRNA gene of *Schistosoma mansoni*, Mol. Biochem. Parasitol. 45 (1991) 205-214.

[25] H. Fujiwara, H. Ishikawa, Molecular mechanism of introduction of the hidden break into the 28S rRNA of insects: implication based on structural studies, Nucleic Acids Res. 14 (1986) 6393-6401.

[26] A. M. Anger, J. P. Armache, O. Berninghausen, et al., Structures of the human and *Drosophila* 80S ribosome, Nature 497 (2013) 80-85.

[27] C. L. N. Ross, R. R. Patel, T. C. Mendelson, V. C. Ware, Functional conservation between structurally diverse ribosomal proteins from *Drosophila melanogaster* and *Saccharomyces cerevisiae*: fly L23a can substitute for yeast L25 in ribosome assembly and function, Nucleic Acids Res. 35 (2007) 4503-4514.

[28] A. Chenuil, M. Solignac, M. Bernard, Evolution of the large-subunit ribosomal RNA binding site for protein L23/25, Mol. Biol. Evol. 14 (1997) 578-88.

[29] S. Metzenberg, C. Joblet, P. Verspieren, N. Agabian, Ribosomal protein L25 from *Trypanosoma brucei*: phylogeny and molecular co-evolution of an rRNA-binding protein and its rRNA binding site, Nucleic Acids Res. 21 (1993) 4936-4940.

[30] J. Azpurua, Z. Ke, I. X. Chen, et al., Naked mole-rat has increased translational fidelity compared with the mouse, as well as a unique 28S ribosomal RNA cleavage, Proc. Natl. Acad. Sci. USA. 110 (2013) 17350-17355.

[31] K. Nishimura, H. Ashida, T. Ogawa, A. Yokota, A DEAD box protein is required for formation of a hidden break in *Arabidopsis* chloroplast 23S rRNA, Plant J. 63 (2010) 766-777.

[32] E. Evguenieva-Hackenberg, Bacterial ribosomal RNA in pieces, Mol. Microbiol. 57 (2005) 318-25.

[33] T. Urakawa, P. A. Majiwa, Physical and transcriptional organization of the ribosomal RNA genes of the savannah-type *Trypanosoma congolense*, Parasitol Res. 87 (2001) 431-438.

[34] G. J. Melen, C. G. Pesce1, M. S. Rossi, A. R. Kornblihtt, Novel processing in a mammalian nuclear 28S pre-rRNA: tissue-specific elimination of an 'intron' bearing a hidden break site, EMBO J. 18 (1999) 3107-3118.

[35] M. N. Schnare, M. W. Grayt, Sixteen discrete RNA components in the cytoplasmic ribosome of *Euglena gracilis*, J. Mol. Biol. 215 (1990) 73-83.

[36] G. Lenaers, L. Maroteaux, B. Michot, M. Herzog, Dinoflagellates in Evolution. A molecular phylogenetic analysis of large subunit ribosomal RNA, J. Mol. Evol. 29 (1989) 40-51.

[37] P. H. Doer, M. W. Gray, Scrambled Ribosomal RNA Gene Pieces in *Chlamyclomonas reinhardtii* Mitochondrial DNA, Cell 55 (1988) 399-411.

[38] D. F. Spencer, J. C. Collings, M. N. Schnare, M. W. Gray, Multiple spacer sequences in the nuclear large subunit ribosomal RNA gene of *Crithidia fasciculata*, EMBO J. 6 (1987) 1063-1071.

[39] D. A. Campbell, K. Kubo, C. G. Clark, J. C. Boothroyd, Precise identification of cleavage sites involved in the unusual processing of Trypanosome ribosomal RNA, J. Mol. Biol. 196 (1987) 113-124.

Figure legends

Fig. 1. *S. marmorata* **silk gland ribosomal translation function.** (A) poly(U)-dependent polyphenylalanine synthesis. Ribosomes (10 pmol) from silk glands of seasonally collected *S. marmorata* larvae were incubated with *B. mori* translation elongation factor mix (EF-mix) for 10 min; radioactivity of the incorporated [^{14}C] phenylalanine was measured as described in Materials and Methods. Dissected silk glands were pre-treated via (i) immediate freezing in LN$_2$ or (ii) immersion in ice-cold saline for several hours (Fig. S1). For comparison, *B. mori* silk gland ribosomes were similarly analyzed. (B) 8 M urea extracts of insoluble cell residues (S10) from winter/LN$_2$ (lane 1) and summer/ice-cold (lane 2) silk glands were analyzed on 3–20 % (w/v) SDS-PAGE.

Fig. 2. Ribosome sedimentation profiles. Purified ribosomes (10 pmol) were ultracentrifuged over a 15%–30% (w/v) sucrose gradient under low (A) or high (B) ionic strength conditions; A$_{260}$ of the gradient was continuously measured from the bottom of the tube. Summer and winter *S. marmorata* ribosomes are indicated by red and blue lines, respectively; black dotted line indicates *B. mori* ribosomes.

Fig. 3. Analysis of ribosomal components. (A) Purified (0.3 A$_{260}$ unit) summer/LN$_2$ (lane 1), winter/LN$_2$ (lane 2), and summer/ice-cold ribosomes (lane 3) were subjected to 16.5 % (w/v) SDS-PAGE; protein components were visualized with CBB staining. (B) Phenol-extracted rRNAs (250 ng) from active ribosome samples of *R. norvegicus* (Rn), *B. mori* (Bm), and *S. marmorata* (Sm) were separated on 1% agarose gel electrophoresis under denaturing (left) or natural (right) conditions; the gel was stained with SYBR Gold.

Fig. 4. Comparison of the region around the 28S rRNA central hidden break.
Secondary structures of the ES19L-containing 28S rRNA regions of *S. marmorata* (A)
and *B. mori* (B) were constructed using 2D and 3D cryo-electron microscopy data from
D. melanogaster (C) and *H. sapiens* (D) [26]. *B. mori* 28S rRNA nucleic acid sequence
was acquired from RNA-seq assembly data (BomoMG comp40229 c0 seq1) in
SilkBase (http://silkbase.ab.a.u-tokyo.ac.jp). (E) Amino acid sequence alignment of
L23a ribosomal proteins from *S. marmorata* (Sm), *B. mori* (Bm), *D. melanogaster*
(Dm), and *H. sapiens* (Hs). Asterisks and periods indicate conserved residues across all
four and three species, respectively. The region visualized in cryo-electron microscopy
[26] is shown in the bold-line box. Accession numbers for the L23a amino acid
sequences are as follows: *B. mori* (AAV34835.1), *D. melanogaster* (NP_523886.1),
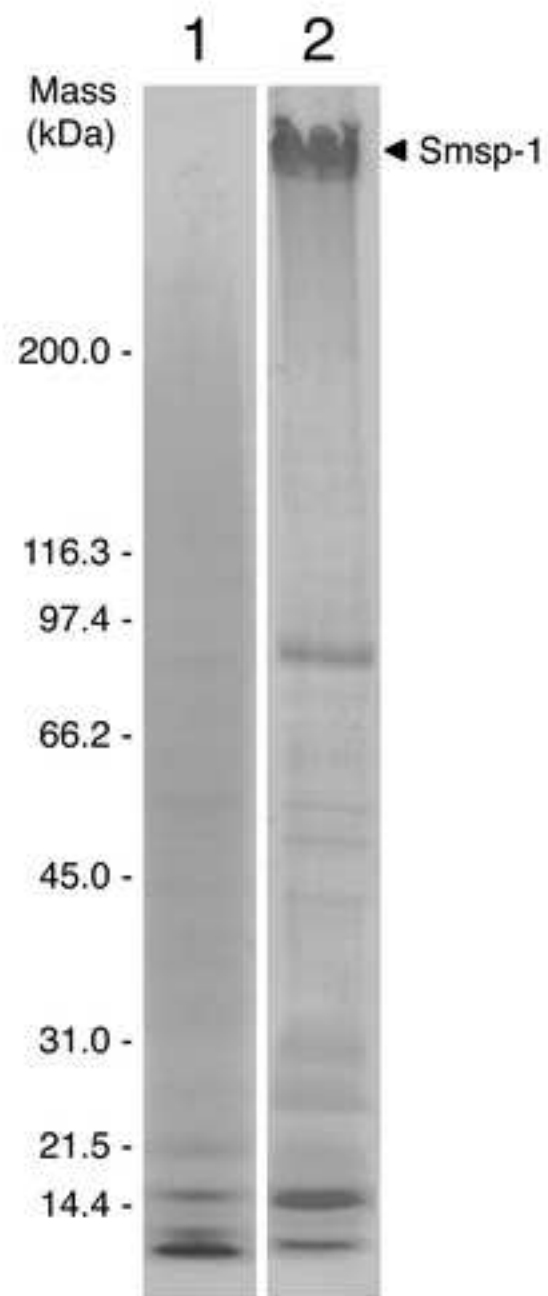and *H. sapiens* (NP_000975.2).

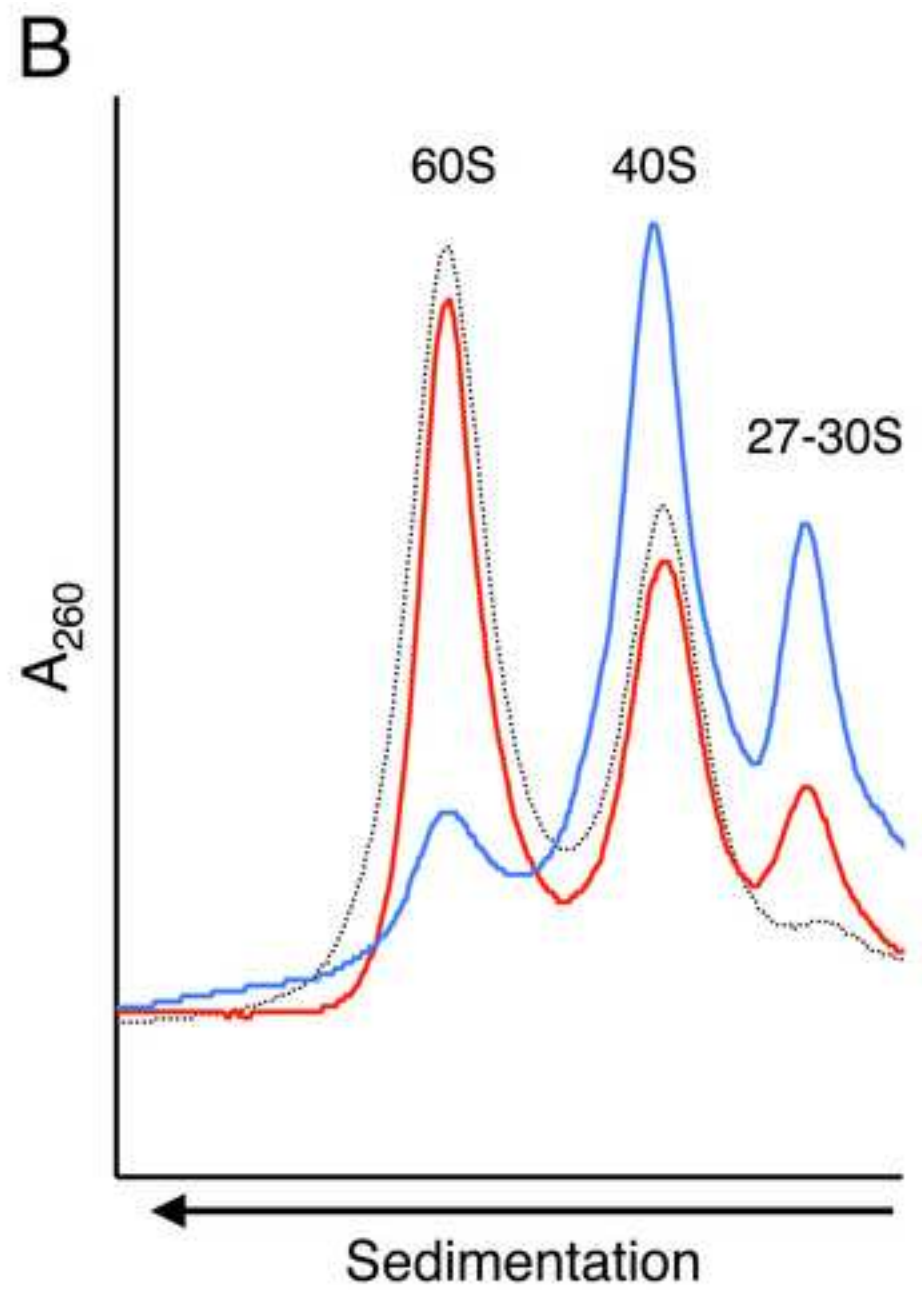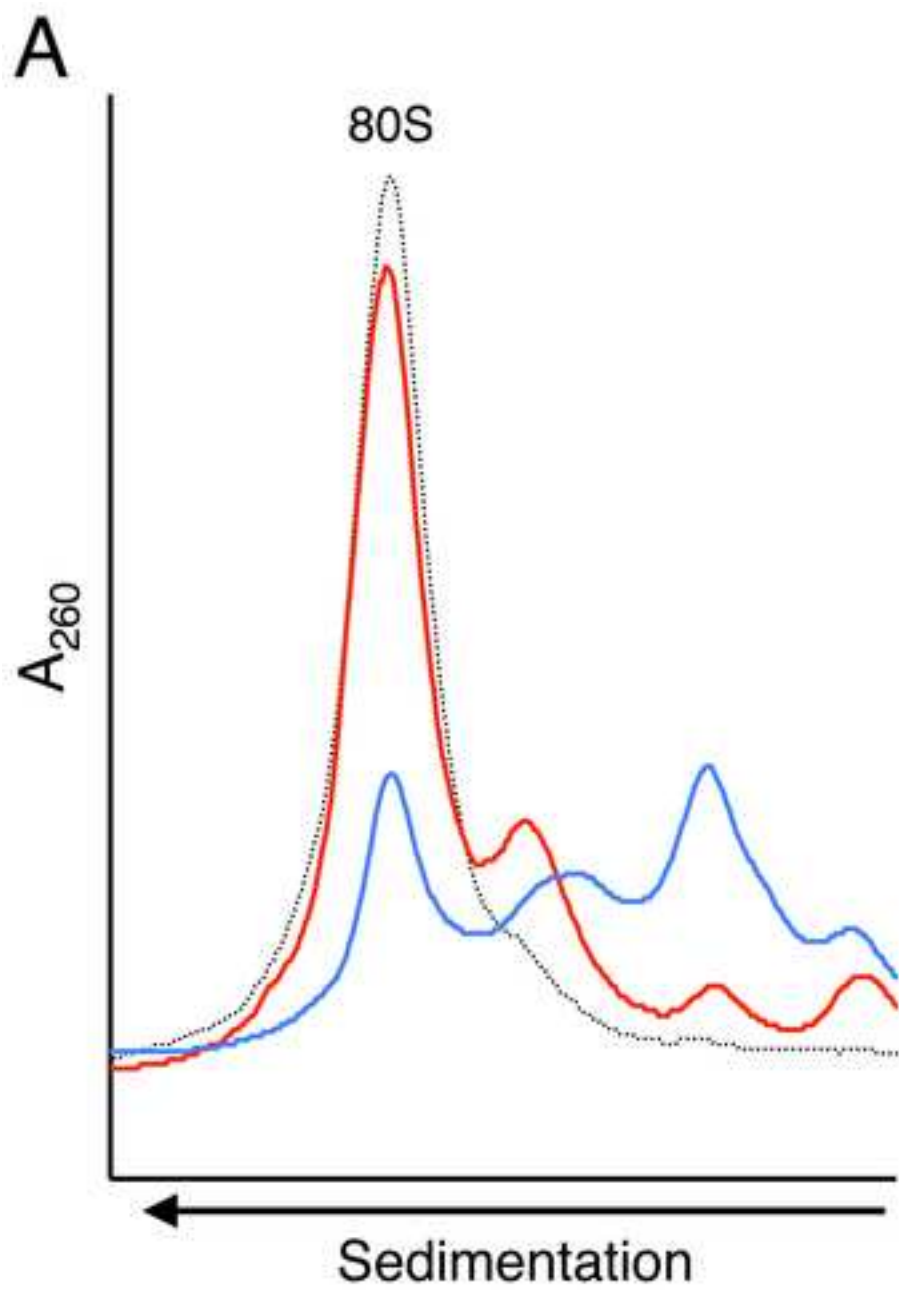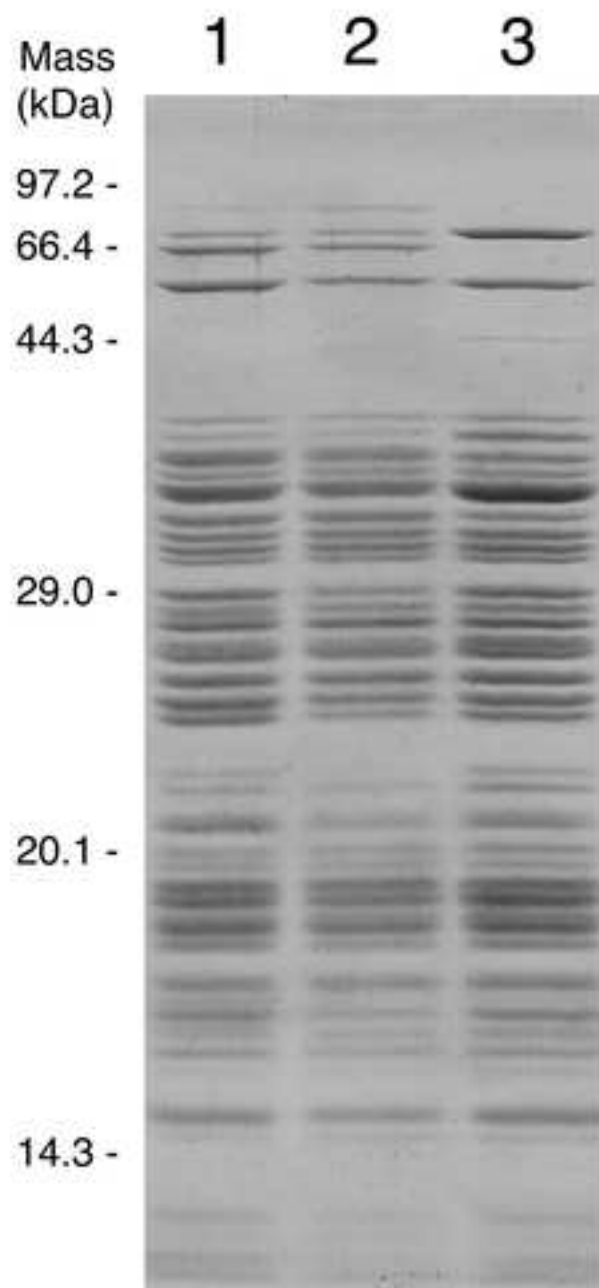**Figure 1_Nomura**
Click here to download high resolution image

A

Mass (kDa)

97.2 -
66.4 -
44.3 -
29.0 -
20.1 -
14.3 -

1 2 3

B

native   denaturing

Rn Bm Sm   Rn Bm Sm

◁ 28S
◁ 18S
◁ 5 / 5.8S

A

predicted splice site

ES19L (D7a)

S. marmorata (caddisfly)

B

31 bases spliced out

28S α   28S β

B. mori (silkworm)

C

45 bases spliced out

28S α   28S β

D. melanogaster (fruit fly)

D

H. sapiens (human)

E

```
Sm   1 MPPKKPADKPAS-GSKASEAKKPKT-EAKAEAPKAEAKPAAAKATT----SKGPAAKPAEKKPADKPKAETKSKVAEAPKLPDKSKAEKAKAADKAKAAPAAAKAKPAAAKKAGDKKPAAKPADKAKAGD 124
Bm   1 MPPKKQPEKSGSSGSKPAEKKP-ATAKTPAAAPKAAAAPAASASSTKPASAKTPAPAPKAAAPAPKPAAPAPKPAAPAPKAASAPKAA-ASAPKPAAPAPKPAAAKPAAAKPAAAKPAAAKPAAAKPAAA 128
Dm   1 MPPKKPTEKSAKPGDKKPEQKK--TAAAP-AAGKKEAAPSAAKP------------------A-------AAAPKKA--------------AAPAAKKAAPAAK-----KPATAGAAAAKKPAAV  77
Hs   1 MAPKAKKEAPAP-------------------PKAEA------------------------------------------------------------------------------------ 17
       * *** . .. ..     . .  . . .        . .     . .*.**       . ...        ..   . ....    .    .    .    +
```

```
Sm 125 KPKAAAKPKAGEKA--KAGD--KK------------------A----------VAKKAAAPKAAKT--PKADAAKAKLAAKV-----KKAAPVKGKSGVK-LTIAKARKAQIKIIKGEHGTRERKIRTSVHFR 217
Bm 129 KPAA------AAAAAPTSKPAEKKTASAPTAKPGSAKAAALKAKSSAKPSAKKAA-ATAAKTAKPKPAVSKLKIAPKP------KK-TGIKGQKKVV-KPVTKALKAQRKVVKGEHGKRVRKIRNSVHFR 243
Dm  78 KTTA------AAKA--KSKDAKKKVLAGKKPQSV----------------------LAKLSAKARAAAKAKKGVKPVT-KPAKGTAKAKAVALLNAKKVQKKIIKGAFGTFARKIRTNVHFR 168
Hs  18 ----------------------------------------------------------------------------KAKALKAKKAVLKGVHSHKKKKIRTSPTFR 47
        .    .    ..   . .      ..          .   .  .             . .         ..    . .  .  .. .  .  ** .. . *** ... **
```

```
Sm 218 RPKTFRPPRNPKYQRNSVSKRTRMDAYNIIKFPLTSEAAMKKIEDNNTLVFIVHTRSNKHHIRQAVKKLYDINVAKVNTLIRPDGKKKAYVRLARDYDALDVANKIGII                    326
Bm 244 RPKTFEPPRRHPKYPRKSLPKRNRMDAYNIIKFPLTSEAAMKKIEDNNTLVFIVHTSANKHHIKAAVKKLYDINVAKVNTLIRPDGKKKAYVRLARDYDALDVANKIGII                    352
Dm 169 RPTTLKLPRSPKYPRKSVPTRNRMDAYNIIKYPLTTEAAMKKIEDNNTLVFLTHLRANKNHVRAAVRKLYDIKVAKVNVLIRPDGQKKAYVRLARDYDALDIANKIGII                    277
Hs  48 RPKTLRLRRQPKYPRKSAPRRNKLDHYAIIKFPLTTESAMKKIEDNNTLVFIVDVKANKHQIKQAVKKLYDIDVAKVNTLIRPDGEKKAYVRLAPDYDALDVANKIGII                    156
        **.* .   * ***.*.* .    ***.*** ***. *.*********** ... .**  .  ** *** *** ***** ****** ******** ****** *******
```